Rare Metal Materials and Engineering
Volume **, Issue **, ***
Available online at **www.rmme.ac.cn**

Science Press

Cite this article as: Rare Metal Materials and Engineering,.

ARTICLE

DOI: 10.12442/j.issn.1002-185X.E20240568

Effect of Rare Earth on Microstructure and Properties of Deposited Metal in Submerged Arc Welding of 1000MPa Grade High Strength Steel

Li Chunjian[1, 2], Xu Kai[1, 2], Feng Wei[1], Song Changhong[1], Zhang Qingsu[1], Hao Qianyu[1], Zheng Yongqiang[1], Guo Xuchao[3]

[1] Harbin Well Welding Co., Ltd., Harbin 150000, China; [2] Harbin Welding Institute Co., Ltd., China Academy of Machinery Science and Technology Group Co.,Ltd, Harbin 150028, China; [3] Suzhou Space Pioneer Co., Ltd., Suzhou 215637, China

Abstract: The application of 1000 MPa grade high-strength steel in the hydropower sector has become increasingly mature, yet there is a paucity of research and development on corresponding high-performance welding materials domestically. Achieving a balance between high strength and toughness in the deposited metal is a critical challenge in the development of such welding materials. Addressing this issue, this paper explores the optimization of deposited metal properties through the addition of rare earth elements to welding materials. Utilizing analytical methods such as OM, SEM, EDS, and XRD, combined with software tools like Matlab, IPP, and CHANNEL5, the study investigates the influence mechanism of rare earth elements addition on the strength, toughness, and inclusions of deposited metal in 1000 MPa grade high-strength steel. The results indicate that the incorporation of rare earth elements enhances the weldability of the welding materials. With the addition of rare earth, the tensile strength of the deposited metal increases from 935 MPa to 960 MPa; however, further addition leads to a decrease in tensile strength, while the yield strength continuously increases by 8.5% to 17.2%. The addition of appropriate amounts of rare earth results in an increase in acicular ferrite and retained austenite content, as well as grain refinement in the deposited metal, leading to an 8.5% to 24.3% increase in impact energy at -40 ℃ and a 15.6% to 42.2% increase at -60 ℃. Additionally, the proper addition of rare earth modifies the inclusions, generating fine, dispersed composite inclusions that bond better with the matrix, thereby optimizing the properties of the deposited metal through various mechanisms. By adding an appropriate amount of rare earth, the properties of the deposited metal in 1000 MPa grade high-strength steel can be significantly enhanced, improving the match between high strength and toughness, and meeting the demands for high-strength steel used in hydropower applications.

Key words: 1000MPa Grade High-Strength Steel; Deposited Metal; Submerged Arc Welding; Rare Earth; Inclusions.

Hydropower is characterized by its environmental friendliness, significant economic benefits, outstanding social comprehensive benefits, stable and secure energy supply, mature and reliable technology, as well as its contribution to ecological and environmental protection. It has played a crucial role in promoting China's green economic development. To enhance the capacity of hydroelectric generation, domestic and international hydropower institutions have continuously increased the rotation speed, efficiency, and capacity of generator sets. This, in turn, has raised higher requirements for the performance of steel used in penstocks, fins, branch pipes, spiral cases, and other components in hydropower stations[1,2]. In order to meet the layout of hydropower stations, reduce the weight and wall thickness of penstocks and spiral cases, improve the welding performance of welded joints, and lower overall project costs, the construction of hydropower stations has progressively adopted higher strength grade steels, advancing from the early 500 MPa grade to the 1000 MPa grade. Japan has already applied 1000 MPa grade high-strength steel in the Kanagawa hydropower station, significantly enhancing

Received date:
Foundation item:Provincel Key Research and Development Plan of Heilongjiang (2022ZX04A01)
Corresponding author: Xu Kai, Professor, Harbin Welding Institute Co., Ltd., China Academy of Machinery Science and Technology Group Co.,Ltd, Harbin 150028, P. R. China, Tel: 0451-86333949, E-mail: xkwelding@163.com

equipment stability and reducing construction costs[3,4]. However, its application in domestic hydropower facilities is relatively limited, indicating a significant gap compared to countries that have mastered this technology. To address this, Baotou Groups in China has developed 1000 MPa grade steel for hydropower use and achieved mass production across various thicknesses. Nevertheless, there is a paucity of research on corresponding welding materials, with the matching of high strength and toughness in deposited metal remaining a challenge in welding material development.

Rare earth elements (REEs), as important additives in the metallurgical industry, exhibit great potential in improving the microstructure and comprehensive properties of steel materials due to their unique physicochemical properties. Since the High-Alloy Stainless Steel produced by Carpenter Company and the steel casting by American Steel Foundries in the early 1950s, REEs have attracted considerable global interest[5,6]. In recent years, numerous reports have documented the application of REEs in HSLA (Low Alloy High Strength) to enhance their toughness[7-11], and research on improving weldability has also been reported. For instance, Baotou Groups has used REEs in Q690CF to reduce carbon equivalent and welding crack sensitivity index, thereby enhancing the weldability of HSLA[12]. However, the application of REEs in welding materials for 1000 MPa grade high-strength steel is rarely explored, and systematic research on the microstructure and properties of submerged arc welding deposited metal is scarce.

Therefore, this study aims to optimize the submerged arc welding materials for 1000 MPa grade high-strength steel using REEs. Through performance tests, microstructural observations, and statistical analysis of inclusions, the mechanisms of REEs' influence on the strength, toughness, and inclusions in deposited metal are investigated using OM (Optical Microscope), SEM (Scanning Electron Microscope), and EBSD (Electron BackScatter Diffraction). This research provides support for both REE research and practical engineering applications.

1 Experiment

The test steel plate was made of Q235 material, with dimensions of 350 mm × 300 mm × 20 mm. A 45° V-shaped groove was cut, and the bottom gap of the test plate was set to 16 mm. A backing plate of 350 mm × 30 mm × 10 mm was placed at the bottom of the test plate. The base welding was performed using J107S, a 1000 MPa grade high-strength steel electrode produced by Harbin Well Welding Co., Ltd. A 4 mm transition layer was deposited on the surface of the groove. The schematic diagram of the welded test plate is shown in Fig 1. The welding process parameters are presented in Table 1.Through experimentation, these are found to be the optimal process parameters[13].

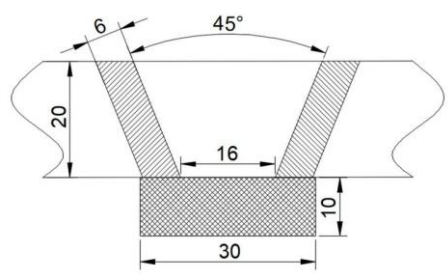

Fig.1 Schematic Diagram of Welded Test Plate

Table 1 Welding Process Parameters

Welding Current I/A	Arc Voltage U/V	Welding Speed v/(cm·min^{-1})	Interlayer Temperature T_0/℃	Postheating Temperature T_1/℃
450	32	40	≤200	350

For the welding material, the self-developed 1000 MPa grade high-strength steel submerged arc welding wire HW-100S from Weier was used to weld the test plate. The welding wire had a diameter of ϕ3.2 mm. Following the design concepts of purification and low carbonization, it had low contents of P and S and incorporated elements such as Cr, Ni, Si, Mn, Ti, and Mo, meeting the requirements for high strength and toughness matching of the deposited metal. The composition of the welding wire used is shown in Table 2.

Table 2 Composition of 1000MPa Grade High-Strength Steel Welding Wire (Mass Fraction, %)

C	Si	Mn	S	P	Cr	Ni	Mo	Fe
0.12	0.18	1.98	0.003	0.007	0.55	2.78	0.45	Reminder

The welding flux used was a fluoride-alkali type, with strict control over elements such as P, S, and O in the deposited metal. In the composition of the flux, CaF_2 plays a key role in slag formation. It effectively reduces the melting point, viscosity, and surface tension of the slag, enhancing its fluidity and reducing gaseous impurities in the weld metal. This aids in the release of gases from the weld and has a certain dehydrogenation effect, reducing the diffusible hydrogen content in the weld[14]. MgO increases the alkalinity of the flux, thereby enhancing the impact toughness of the weld metal and significantly affecting the welding process performance[15]. SiO_2 reduces the alkalinity of the flux and synergistically works with CaF_2 to influence the flux's resistance to porosity and corrosion. The acicular and fibrous crystal morphology of wollastonite in the flux increases particle strength and reduces particle fragmentation[16]. Al_2O_3 has the effect of increasing the surface tension of the molten slag and is an adjuster for slag viscosity and flux alkalinity[17]. CaO is a major component of the molten slag. It regulates the alkalinity of the slag and effectively enhances the flux's ability to withstand high currents, improving the sur-

face tension and interfacial tension of the molten slag[18]. TiO_2 improves the viscosity and interfacial tension of the molten slag, promoting the discharge of the slag system during welding[19]. MnO combines with SiO_2 during welding to form complex silicates, generating good weld slag to protect the weld from the influence of N and O in the air. The reduced Mn element enhances the strength and impact toughness of the weld, compounds with S in the weld to form MnS, which acts as a desulfurizer, thereby reducing the tendency for hot cracking. To facilitate the rapid escape of gases during welding, ensure welding process performance, and obtain a weld with a smooth and aesthetically pleasing surface, the flux particle size was set to 10-60 mesh. In summary, the main components of the flux are shown in Table 3. Rare earth elements were introduced into the deposited metal by adding 40-mesh rare earth fluorides with a purity greater than 99.95% to the flux. The designed rare earth addition amounts are shown in Table 4.

Table 3 Composition of 1000MPa Grade High-Strength Steel Welding Flux (wt%)

Ingredients	CaF_2	SiO_2	MgO	TiO_2	Al_2O_3	CaO
Content	20-28	5-8	18-21	5-8	16-24	16-22

Table 4 Amount of Rare Earths Added to the Welding Flux (Parts)

Number	1	2	3	4
Type	No Rare Earth	Rare Earth	Rare Earth	Rare Earth
Addition Amount	0	1	2	4

The welded plate was sampled according to the method shown in Fig 2. Tensile test speciments were prepared in accordance with the standard GB/T 228.1-2021 "Metallic Materials - Tensile Testing - Part 1: Method of Test at Room Temperature" and tested on a UTM5305SYXL electronic tensile testing machine. Impact test speciments for temperatures of -40 °C and -60 °C were prepared in accordance with the standard GB/T 229-2020 "Metallic Materials - Charpy Pendulum Impact Test Method", with three speciments prepared for each temperature. These speciments were tested on a JBN-300B impact testing machine using the Charpy V-notch impact test method. In accordance with the standard GB/T 223.92-2023 "Determination of Lanthanum, Cerium, Praseodymium, Neodymium, and Samarium Content - Inductively Coupled Plasma Mass Spectrometry Method", deposited metal powder was drilled from a depth of 1/2 of the weld bead. The powder and the rare earth components in the prepared flux were analyzed using ICP-MS (Inductively Coupled Plasma Mass Spectrometry) on an ICAP6300 Radial instrument. The direct-read speciment was processed into a metallographic speciment through wire cutting and hot mounting. After grinding and polishing, 100 images were randomly taken at 1000x magnification using an OLYMPUSGX51 optical microscope. The inclusions were analyzed using IPP software (Image-Pro Plus). The metallographic speciment was then chemically etched with a 2.5% nitric acid alcohol solution and observed under an optical microscope to examine the metallographic structure of the deposited metal. The fracture morphology and high-magnification metallographic structure of the -60°C low-temperature impact test speciment were observed using a Hitachi SU5000 scanning electron microscope. For EBSD speciments, after grinding and polishing, electrolytic polishing was performed using a solution of 10% perchloric acid + 90% glacial acetic acid. The speciments were then observed using an electron microscope with a scanning step size of 0.1 μm.After polishing, the sample was analyzed for phase composition using an X'Pert PRO X-ray diffractometer (XRD) with a Cu target and a scanning rate of 2°/min.

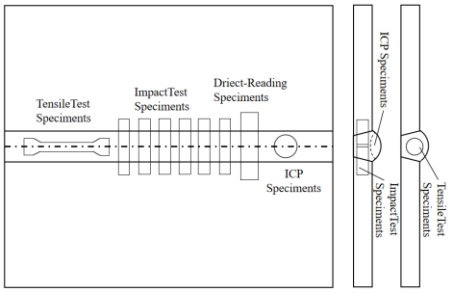

Fig.2 Schematic Diagram of Sampling Locations

2 Results and Discussion

2.1 Weldability and Mechanical Properties

The appearance of the deposited metal weld beads is shown in Fig.3, where Fig.3a to Fig.3d correspond to test plates 1 to 4, respectively, and the welding process parameters are presented in Table 5. Both before and after the addition of rare earth elements, the welding materials exhibited excellent processability, with no splashing during the welding process. The deposited metal was straight and smooth, without issues such as undercut, slag inclusion, or pits. The mechanical properties of the deposited metal from the submerged arc welding of 1000 MPa grade high-strength steel with different rare earth contents are shown in Table 6, and the strength-toughness relationship of the deposited metal is illustrated in Fig.4. When the rare earth addition was 1 part, there was no significant change in tensile strength, which remained around 930 MPa, while the yield strength increased from 740 MPa to 820 MPa, representing a 10.8% increase. Upon further increasing the rare earth addition to 2 parts, the tensile strength and yield strength increased by 2.7% and 17.2%, respectively. When the addition reached 4 parts, the tensile strength decreased by 5.3% compared to the unadded case, but the yield strength still increased by 8.5% compared to the unadded case. The

low-temperature toughness of the 1000 MPa grade high-strength steel deposited metal was overall enhanced after rare earth treatment, but the increase first rose and then declined, with an 8.5% to 24.3% increase in impact energy at -40 ℃ and a 15.6% to 42.2% increase at -60 ℃. Therefore, the mechanical test results indicate that rare earths can significantly increase the yield strength, lower the ductile-to-brittle transition temperature of the deposited metal, and enhance the overall toughness. The optimal rare earth addition is 2 parts, which ensures a good strength-toughness match. With a tensile strength of 950 MPa meeting engineering requirements, the impact absorption energy at -60 ℃ reached over 75 J, far exceeding engineering specifications.

Fig.3 Appearance of the Deposited Metal Weld Bead

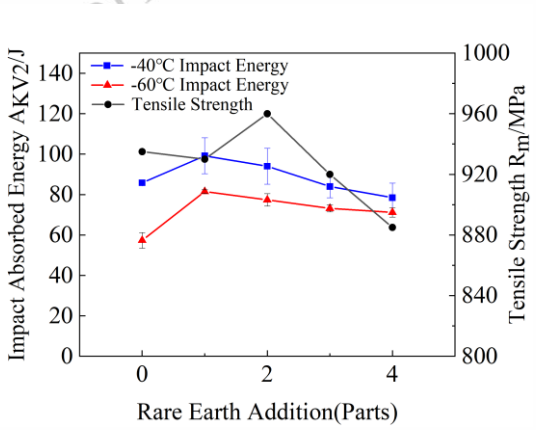

Fig.4 Strength and Toughness of Deposited Metal with Different Rare Earth Contents

Table 5 Welding Process Properties

Plate Welding Code	Welding Process Properties
1	During the welding process, there is no spatter, the slag removal effect is good, and there are no issues such as undercut, slag inclusion, or pits
2	During the welding process, there is no spatter, the slag removal effect is good, and there are no issues such as undercut, slag inclusion, or pits
3	The slag removal is favorable, the slag shell is intact, and the oxidation color is relatively heavy
4	The slag removal for the first two layers is poor, but it improves as the number of layers increases, and the oxidation color is relatively heavy

Table 6 Mechanical Properties of Deposited Metal with Different Rare Earth Contents

Number	Tensile Strength	Yield Strength	Elongation	-40 ℃ Impact Energy			-60 ℃ Impact Energy		
	R_m/MPa	$R_{p0.2}$/MPa	A(%)	A_{KV2}/J			A_{KV2}/J		
1	935	740	16.0	87	86	86	53	59	61
2	930	820	19	103	106	89	81	82	82
3	960	867	15.5	86	104	93	74	80	78
4	885	803	18.5	85	81	71	72	69	73

2.2 Chemical Testing

The ICP testing of the deposited metal and the direct reading results are shown in Table 7. It can be observed that most alloy elements did not change significantly after the addition of rare earth elements, the S (Sulfur) content increased slightly, and there was no significant change in O (oxygen). Some

scholars[20] have proposed through thermodynamic calculations that REEs have a greater affinity for O than S and will preferentially combine with O to form inclusions, which can weaken the desulfurization effect. During the welding process of speciment 3, a relatively sufficient metallurgical reaction occurred between the REEs and O, resulting in a heavier oxidation color on the weld bead. Chemical testing also showed a higher content of S element, which affected the corrosion resistance of the speciment and prolonged the corrosion time during the preparation of metallographic speciments by 20%. From the ICP testing results, it can be found that the proportion of REEs present in the deposited metal is the same as the added amount, indicating that the transition of REEs is relatively stable. However, to achieve better mechanical improvement effects, it is necessary to adjust the process parameters to increase the transition coefficient.

Table 7 Chemical Composition (wt%)

Number	C	Si	Mn	P	S	Cr	Ni	Mo	O	Re
1	0.078	0.17	1.8	0.010	0.0023	0.41	2.64	0.69	0.03	0
2	0.075	0.14	1.87	0.012	0.0030	0.46	2.81	0.75	0.03	0.000076
3	0.086	0.14	1.82	0.012	0.0036	0.44	2.75	0.68	0.03	0.00012
4	0.073	0.12	1.86	0.012	0.0031	0.45	2.85	0.77	0.03	0.00025

2.3 Deposited Metal Microstructure

The microstructure of the deposited metal is depicted in Fig.5. Through a comparative analysis of the microstructures, it is evident that REEs do not significantly alter the microstructural composition of 1000 MPa grade low-alloy high-strength steel. Both microstructures primarily consist of F (Ferrite), B (Bainite), and M-A constituents. Ferrite includes blocky PF (proeutectoid ferrite) and AF (Acicular Ferrite). The AF, benefiting from its interlocking structure, effectively impedes crack propagation. Additionally, AF can completely encapsulate particles of non-metallic inclusions traditionally regarded as harmful, thereby significantly reducing or even eliminating the detrimental effects of these inclusions on the material's plasticity and toughness. Increasing the proportion of AF is a key method for enhancing the microstructure's toughness. As observed in Fig.5a and 5d, the number of AF significantly increases, and the size of blocky ferrite decreases after the addition of REEs, explaining the enhanced low-temperature impact toughness. According to Fig.5b and 5e, there are numerous fine and dispersed M-A constituents in the microstructure, which can hinder dislocation movement, reduce stress concentration, and impede crack propagation. The impact fracture morphologies of the deposited metal are shown in Fig.5c and 5f. It can be seen that both fracture modes exhibit microporous aggregation-type ductile fractures. A few tear ridges can be found in specimen 1, while specimen 3 displays deeper and denser dimples, indicating superior toughness.

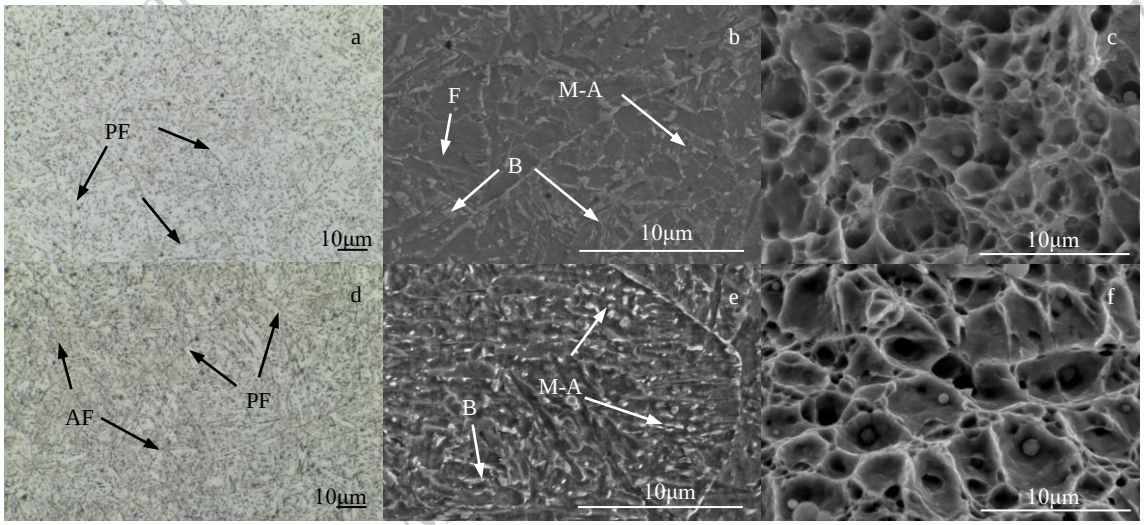

Fig.5 Microstructure of the deposited metal without rare earth treatment (a-c) and with rare earth treatment (d-f).

The microstructure of the deposited metal of 1000 MPa grade high-strength steel with 0, 2, and 4 parts of rare earth addition was analyzed using EBSD. The grain orientation morphology is shown in Fig.7. The scanning location is at the intersection of two weld beads in the weld center. It can be observed that the grains exhibit a typical columnar structure. The grain orientation in speciment 1 and 4 is more pronounced in certain regions, while the orientation in speciment 3 is relatively random. Analysis of the grain boundaries and grains using CHANNEL5 revealed that the proportion of low-angle grain boundaries (2°-15°) is 27% for all three speciments, and the proportion of high-angle grain boundaries (greater than 15°) is 73%, with the majority distributed between 50°-60°, accounting for 62%. The average grain sizes are 1.60 μm, 1.41 μm, and 1.87 μm, respectively, and the average grain areas are 3.99 μm^2, 2.82 μm^2, and 4.93 μm^2, respectively. The proportion of grains of various sizes is shown in Fig.6. It can be seen that after appropriate rare earth treatment of 1000 MPa grade high-strength steel, the proportion of grains smaller than 1 μm increases significantly from 33% to 45%, while the proportion of grains between 1-3 μm decreases. Combined with Fig.7, it can be inferred that the grain size is more uniform and the distribution is more reasonable. However, excessive rare earth addition leads to coarse grains and an increase in large-sized grains, resulting in an initial increase and subsequent decrease in tensile strength. Nonetheless, speciment 4 still exhibits a reduction in the proportion of grains within the 1-3 μm size range, possesses a relatively smaller average grain size, and contains a large number of high-angle grain boundaries. During crack propagation, these features cause crack deflection and blunting, hindering rapid crack propagation. Therefore, speciment 4 retains good low-temperature impact toughness.

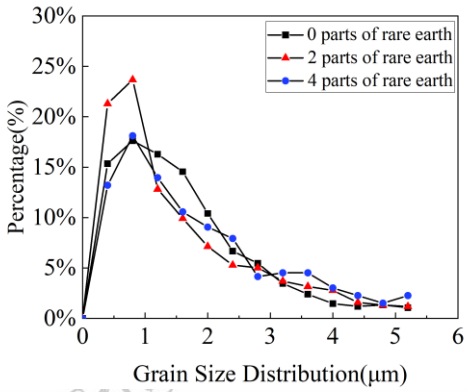

Fig.6 Proportion of Grains of Various Sizes

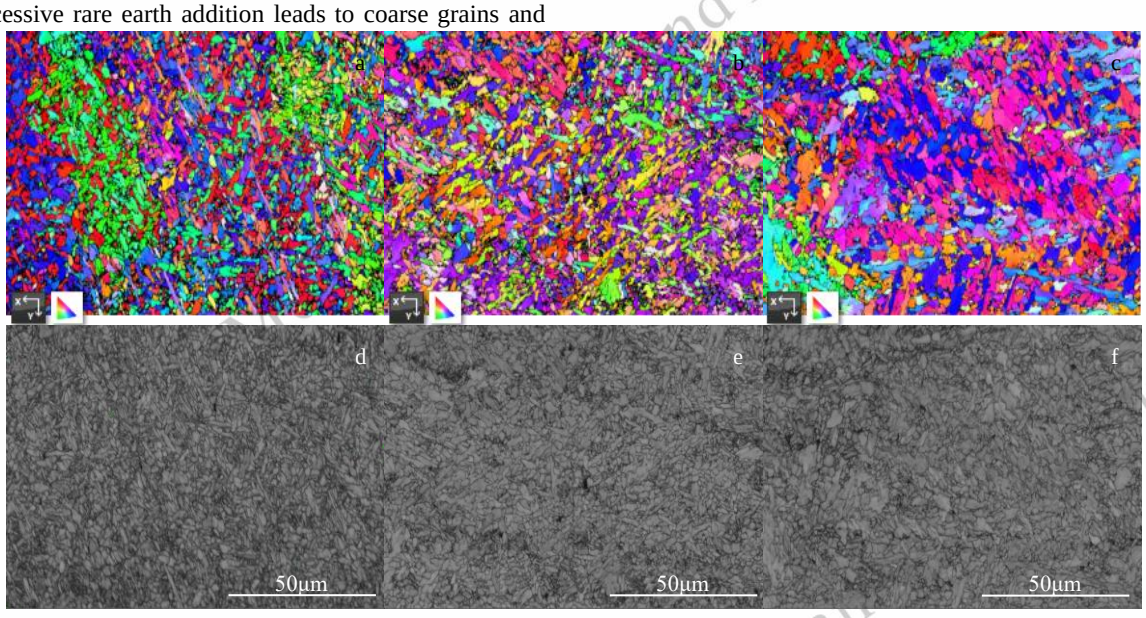

Fig.7 EBSD orientation images of the deposited metal with 0 parts of rare earth (a、 d)、 2 parts of rare earth (b、 e)、 and 4 parts of rare earth (c、 f)

Using the EBSD phase distinction function to analyze the 1000 MPa grade high-strength steel deposited metals before and after rare earth treatment, and combining with the XRD analysis results in Fig.8 and the microstructure morphology shown in Fig.9, it can be observed that the retained austenite is distributed in a diffuse, dot-like manner along the dendrite and grain boundaries. The proportions of retained austenite structures are 0.25%, 0.51%, and 0.41%, respectively. The literature indicates[21,22] that rare earths tend to segregate at austenite grain boundaries, reducing their grain boundary energy and delaying the nucleation of proeutectoid ferrite. This results in a decrease in A_{r3} and A_{r1} during continuous cooling, thereby expanding the austenite phase region and enhancing the stability of austenite. Simultaneously, the solid solution of rare

earths increases the shear resistance of the martensite transformation and lowers the M_s point. Therefore, the retained austenite content is higher in the No.3 and No.4 deposited metals, which contain appropriate and excessive amounts of rare earths, compared to No.1. During impact deformation, the retained austenite undergoes a transformation-induced plasticity effect (TRIP)[23], enhancing the plastic deformation capacity. The formed martensite hard phase particles can serve as a second-phase interface, thereby facilitating the formation of dimples and increasing the crack propagation energy during impact. As the amount of rare earth addition increases, the retained austenite content in the deposited metal first increases and then decreases. There is a competitive relationship between the toughening effect of the austenite ductile phase and the embrittlement effect of the martensite brittle phase in the M-A constituents, which is consistent with the overall improvement and subsequent increase followed by a decrease in the low-temperature impact toughness plateau.

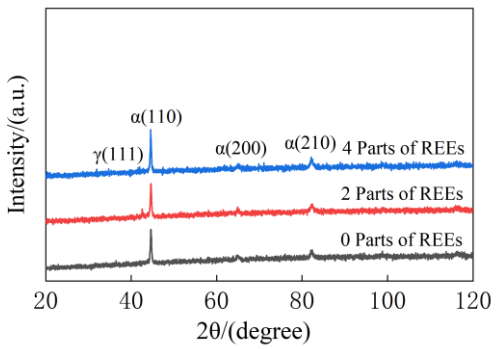

Fig.8 XRD spectra of deposited metals of 1000 MPa grade high-strength steel with different rare earth additions

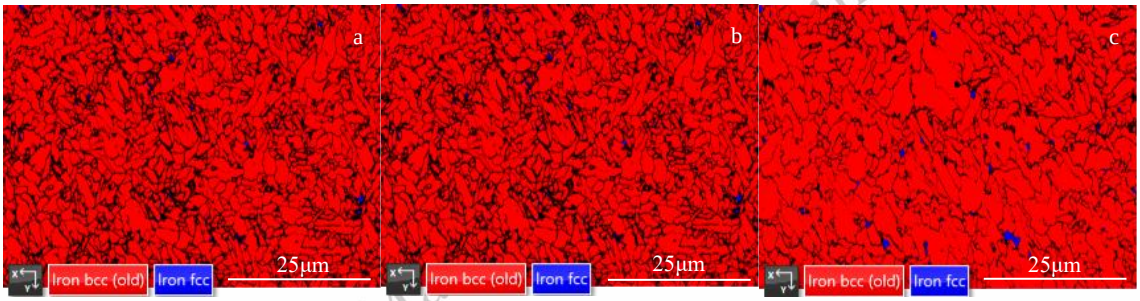

Fig.9 EBSD phase distinction maps of deposited metal with 0 parts of rare earth (a)、 2 parts of rare earth (b)、 and 4 parts of rare earth (c)

Regarding the existence and distribution of REEs in steel, some scholars have pointed out that Ce has a very strong segregation tendency at grain boundaries, significantly higher than that of elements such as S, P, and B. When a small amount of REEs is added to steel, it preferentially forms rare earth inclusions, and the amount of rare earth present in solid solution is relatively small[20]. Therefore, this article uses EDS to analyze grain boundaries and determine the influence of rare earth content on the microstructure and properties of the deposited metal of 1000 MPa grade high-strength steel.

Scanning the grain boundary precipitates of speciment 3 and 4 using EDS, as shown in Fig.10a, when the rare earth content is low, the segregated components include alloy elements such as Ni, Mn, and Cr. Rare earth elements do not accumulate at the grain boundaries but form complex rare earth inclusions within the grains. Fig.10b indicate that as more rare earth is added, REEs begin to precipitate and significantly segregate at the grain boundaries. Scanning multiple precipitates on the impact fracture surface of speciment 4 reveals the presence of REEs, further confirming the phenomenon of significant rare earth segregation. According to the composition of the precipitates listed in Table 8, excessive rare earth can form composite segregates and brittle phases with impurity elements such as S at the grain boundaries, which may become crack sources or crack propagation paths, increasing the crack sensitivity of the deposited metal and reducing its toughness.

Table 8 Composition of grain boundary precipitates

Cr	Mn	Ni	S	Ce
12.73	7.10	52.40	3.83	20.03

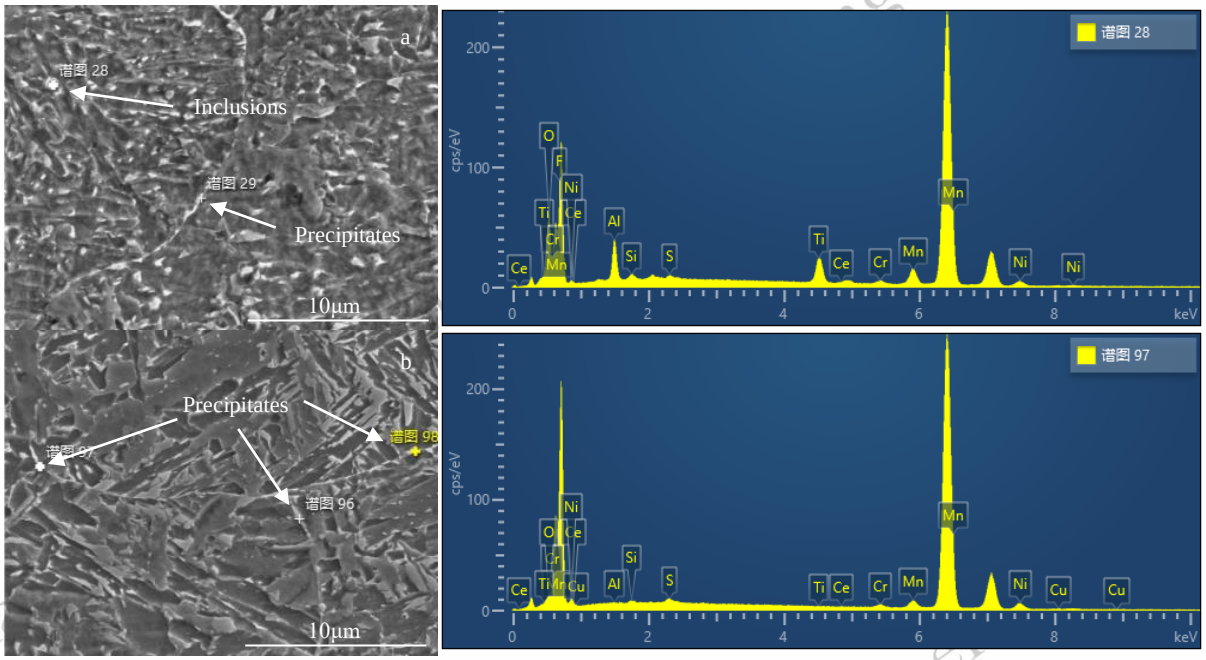

Fig.10 EDS results of grain boundary precipitates

2.4 Inclusion Analysis

In HSLA, inclusion modification is an effective method to increase the amount of AF. Scholars such as Li Zhuoxin[24] have proposed that in HSLA, inclusions with a core mainly composed of MnS and other non-crystalline phases, a size of 0.5-0.8 μm, a volume fraction of 36%, a surface enriched with a 10-20 nm TiO thin layer, and a spherical shape can definitely promote the nucleation of AF. In this paper, observations were made on inclusions of various sizes in the deposited metal of 1000 MPa grade high-strength steel before and after rare earth treatment. The morphology and element distribution of the inclusions under SEM are shown in Fig.11. From Fig.10a and 10b, it can be observed that large-sized inclusions are regularly round, and their composition consists of oxides of Mn, Ti, Si, and Al. The distribution of various metal elements in the inclusions is uniform. In Fig.11a, Si content is relatively low (wt%=0.19) and is present at the center of the inclusion, while in Fig.11b, Si content is higher (wt%=0.39) and is mainly distributed on the outer side of the inclusion. From Fig.11c, it can be seen that small-sized inclusions are rare earth inclusions, and two inclusions grow in parallel with different compositions. The larger one consists of a small amount of REEs, Mn, Ti, Al, and O, with REEs distributed in the innermost layer, surrounded by alloy elements, Mn and Ti located in the middle layer, and Al present in both the middle and outer layers. All three layers are oxides, as schematically shown in Fig.12. The smaller one mainly consists of oxides of Mn, Ti, and Al.

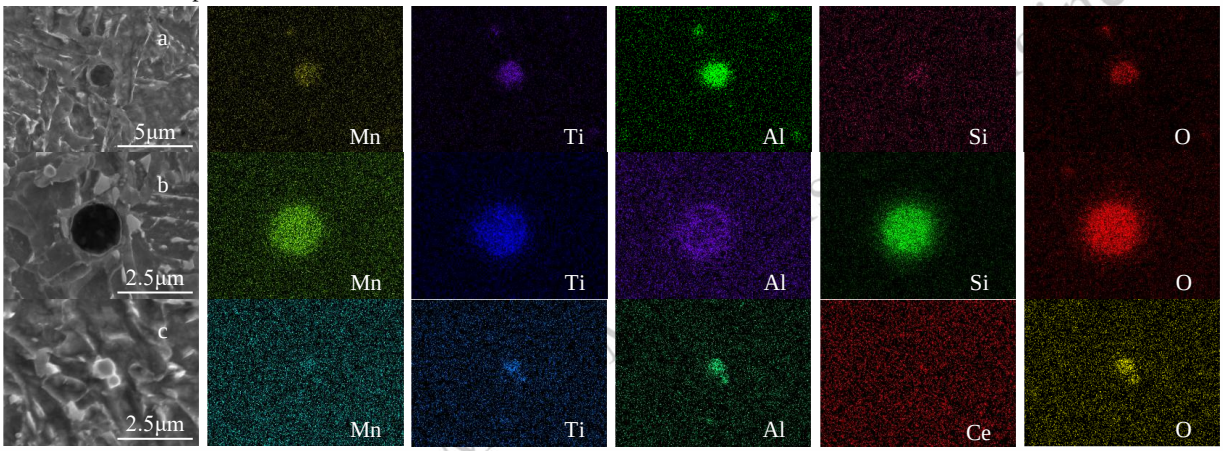

Fig.11 Morphology and Element Distribution of Inclusions of Various Sizes

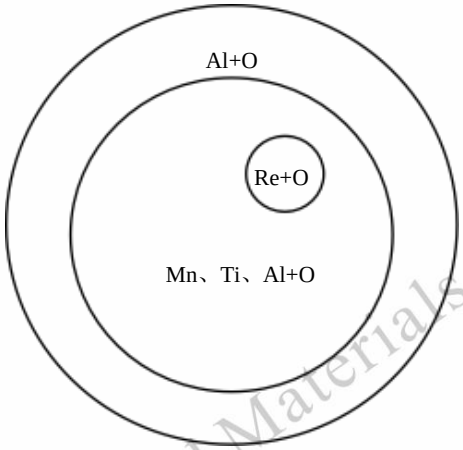

Fig.12 Schematic Diagram of Rare Earth Composite Inclusions

According to the principle of minimum mismatch degree[25], the mismatch degree between composite rare earth inclusions and both α-Fe and γ-Fe is less than 12%. Therefore, they can promote the nucleation of AF and austenite on certain crystal plane families, inhibit the nucleation and growth of non-equiaxed ferrite, and the fine and dispersed rare earth inclusions can also provide more nucleation sites, pin grain boundaries, and refine grains. By scanning the initiation zone, crack propagation zone, and final fracture zone of the impact fracture surface of the deposited metal of 1000 MPa grade high-strength steel treated with REEs, as shown in Fig.13, it can be found that oxides mainly composed of Mn, Cr, Ni, and Al exist in each dimple in the initiation zone, and no REEs are detected. These brittle inclusions become the sources of crack initiation during the impact process. In the crack propagation zone and the final fracture zone, it can be found that REEs begin to exist in large quantities in both the inclusions and the matrix, proving that rare earth inclusions have stronger bonding ability with the matrix compared to common brittle oxide inclusions such as Al_2O_3, and are less prone to causing stress concentration. However, as the stress continues to increase, they can also become paths for crack propagation.

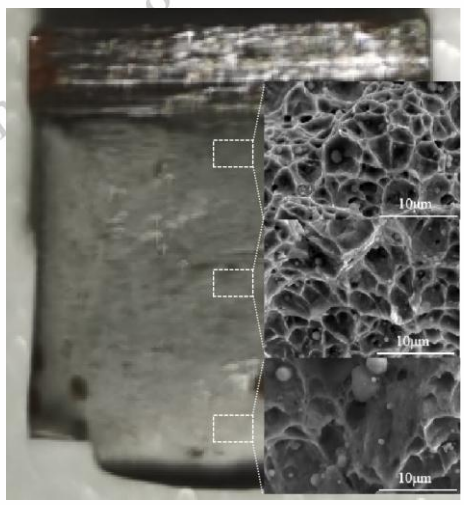

Fig.13 Scanning images of impact fracture surfaces in different regions

To investigate the influence of rare earth content on inclusions in the deposited metal of 1000 MPa grade high-strength steel, software was used to analyze metallographic speciments of deposited metal with 0, 2, and 4 portions of rare earth addition after grinding and polishing, magnified 1000 times under an optical microscope. For each speciments, 100 random fields of view were selected, and validity was determined according to the standard test method specified in GB/T 18876.1-2002 "Standard Test Method for Determining Metallographic Structure, Inclusion Content, and Grade in Steel and Other Metals - Part 1: Image Analysis and Stereological Determination of Inclusion or Second-Phase Structure Content in Steel and Other Metals". At the same time, SEM observations were conducted on the inclusions in the impact fracture surface of each deposited metal, and the results are shown in Fig.14. The average sizes were 0.80μm, 0.77 μm, and 0.79 μm, respectively. The deposited metal with 2 portions of rare earth addition had the highest proportion of inclusions with sizes ranging from 0.6 μm to 0.8 μm, while the proportion of larger-sized inclusions was lower. The correlation coefficient r between the proportion of inclusions of various sizes and the impact toughness at -60 ℃ was calculated using formula (1), and the results are shown in Table 9. It can be inferred that inclusions with sizes ranging from 0.6 μm to 0.8 μm have a highly positive correlation with impact toughness at -60 ℃. Inclusions larger than 0.8 μm and the average size are negatively correlated with impact performance, indicating that small-sized inclusions (0.6-0.8 μm) have a positive effect on improving low-temperature impact toughness. As the amount of rare earth addition increases, the size of inclusions increases, leading to segregation of REEs. The increased size of inclusions and their accumulation at dimples become crack sources, deteriorating performance, thus exerting a negative effect.

$$r(X,Y)=\frac{Cov(X,Y)}{\sqrt{Var[X]Var[Y]}} \quad (1)$$

Table 9 Correlation coefficient r between inclusion sizes and impact properties

0.6-0.8	0.8-1.0	1.0-1.2	1.2-1.4	1.4-1.6	＞1.6	Average Size
0.802	-0.745	-0.867	-0.952	-0.439	-0.938	-0.860

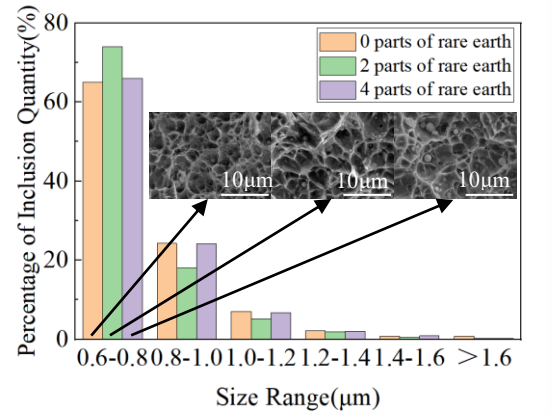

Fig. 14 Correspondence between Inclusion Size Distribution in Deposited Metal of 1000 MPa Grade High-Strength Steel and Morphology of Inclusions in Impact Fracture Surface

3 Conclusions

1) By optimizing the submerged arc welding material for 1000 MPa grade high-strength steel through the addition of REEs, excellent welding workability has been achieved in experiments. The overall mechanical properties of the deposited metal can be enhanced with an appropriate amount of rare earth addition. As the amount of rare earth added increases, the mechanical properties first increase and then decrease. Specifically, the tensile strength improves from 935 MPa to 960 MPa when two portions of rare earth are added, but it drops to 885 MPa with excessive addition. The yield strength increases by 8.5% to 17.2%, and the impact energy at -40 ℃ increases by 8.5% to 24.3%, while at -60 ℃ it increases by 15.6% to 42.2%.

2) When an appropriate amount of REEs is transitioned into the deposited metal, it leads to an increase in AF content, grain refinement, and an increase in retained austenite content, thereby significantly improving the low-temperature impact toughness. However, as the addition amount increases, rare earth segregation occurs, leading to deterioration of grain boundaries, coarse grains, and a decrease in retained austenite content, resulting in a reduction in low-temperature impact toughness. Experiments have determined that the best strength-toughness match for the deposited metal is achieved when two portions of rare earth are added.

3) The proper addition of rare earth can modify the inclusions, producing fine, dispersed composite inclusions that bond better with the matrix. Rare earth inclusions can strengthen the material by inducing the formation of AF nuclei and refining ferrite grains. After rare earth treatment, the average size of the inclusions decreases, and the proportion of inclusions with sizes ranging from 0.6 μm to 0.8 μm increases, which can enhance the impact toughness of the deposited metal. Inclusions larger than 0.8 μm, on the other hand, can reduce its impact toughness.

In summary, welding materials improved with REEs can meet the application requirements for submerged arc welding of 1000 MPa grade high-strength steel in hydropower engineering and can be applied to more working conditions and fields.

References

1 Li Xiaozhu, Chen Zhijun, Fan Xiaochao *et al.* *Renewable and Sustainable Energy Reviews*[J], 2018, 82: 232− 239

2 Pérez-Díaz J I, Chazarra M, García-González J *et al.* *Renewable and Sustainable EnergyReviews*[J], 2015, 44: 767 − 784

3 Horikawa K, Watanabe N. *Welding in the World: Journal of the International Institute of Welding: Journal of the International Institute of Welding*[J], 2008, 52

4 Hara N, Sato M. *Conference on High Strength Steels for Hydropower Plants*[C], Takasaki, Japan, 2009

5 Kippenhan N, Gschneidner Jr K A. *Iowa State Univ. of Science and Technology, Ames. Rare-Earth Information Center*[R], 1970

6 Preinfalk C, Morteani G. *Lanthanides, Tantalum and Niobium: Mineralogy, Geochemistry, Characteristics of Primary Ore Deposits, Prospecting, Processing and Applications Proceedings of a workshop in Berlin, November 1986*[C], Springer Berlin Heidelberg, 1989: 359-370

7 Li Chunlong. *Chinese Rare Earths*[J], 2013, 34(03): 78-85

8 Wang Llifeng, Liu Fengde, Zhang Hong *et al*. *Journal of Mechanical Engineering*[J], 2016, 52(22): 70-77

9 Meng Xianghai, Wang Wei, Bi Sheng *et al*. *Iron and Vanadium*

Titanium[J], 2022, 43(02): 146-151

10 Zang Ruoyu, Li Jing, Huang Fei. *Nonferrous Metals Science and Engineering*[J], 2024,15(03):449-456

11 Gao Huimin, Fang Qi, Sun Wei. *World Nonferrous Metals*[J], 2017(11): 267-269

12 Qin Mu, Yang Xiong, Yang Weiyu. *Science & Technology of Baotou Steel*[J], 2020, 46(02): 52-55

13 Feng Wei, Yu Tingxiang, Xu Kai *et al*. *Welding & Joining*[J], 2023, (11): 6-12

14 Zhang Min, Yao Chengwu, Li Jihong *et al*. *Transactions of the China Welding Institution*[J], 2006, (10): 29-32+114

15 Ding Guangzhu, Guo Weiyun, Wang Shunxing *et al*. *Welding Technology*[J], 2020, 49(05): 90-93

16 Sharma L, Chhibber R. *Ceramics International*[J], 2019, 45(2): 1569 – 1587

17 Sharma L, Chhibber R. *Ceramics International*[J], 2020, 46(2): 1419 –1432.

18 Zhang Wenye. *Welding Metallurgy*[M], Beijing: China Machine Press, 1993

19 He Lei, Wang Renfu, Cheng Yingjin *et al*. *Transactions of the China Welding Institution*[J], 2023, 44(05): 7-13+61+129

20 Geng Ruming. *University of Science and Technology Beijing*[D], 2022

21 Wang Longmei. *Application of Rare Earth Elements in Low Alloy and Alloy Steels*[M], Beijing: Metallurgical Industry Press, 2016

22 Qu Wei, Ren Huiping, Jin Zili *et al*. *Rare Metal Materials and Engineering*[J], 2018, 47(07): 2087-2092.

23 Soleimani M ,Kalhor A ,Mirzadeh H. *Materials Science & Engineering A*[J], 2020,795

24 Li Zhuoxin, Zhang Tianli, Kim H J. *Materials China*[J], 2012, 31(01): 50-55

25 Brammfitt B L. *Metallurgical Transactions*[J], 1970, 1: 1987-1995

稀土元素对 1000MPa 级高强钢埋弧焊熔敷金属组织性能的影响研究

李春剑[1,2]，徐 锴[1,2]，冯 伟[1]，宋昌洪[1]，张庆素[1]，郝乾宇[1]，郑勇强[1]，郭旭超[3]

(1. 哈尔滨威尔焊接有限责任公司，哈尔滨 黑龙江 150000)

(2. 中国机械总院集团哈尔滨焊接研究所有限公司，哈尔滨 黑龙江 150028)

(3. 苏州天兵科技有限公司，苏州 江苏 215004)

摘 要：1000 MPa 级高强钢在水电领域的应用已日趋成熟，但国内相应高性能焊材的研发较少，熔敷金属高强韧性匹配是此类焊材的研发难点。针对此问题，本文通过在焊材中添加稀土元素优化熔敷金属性能，并利用 OM、SEM、EDS、XRD 等分析方法，结合 Matlab、IPP、CHANNEL5 等软件研究了稀土元素添加量对 1000MPa 级高强钢熔敷金属强韧性及夹杂物的影响机理。结果表明：稀土的添加有利于焊材的焊接工艺性；随稀土的添加，熔敷金属抗拉强度从 935 MPa 提高到 960 MPa，继续添加则导致了抗拉强度下降，而屈服强度持续提高 8.5%~17.2%；适量稀土元素的添加使熔敷金属针状铁素体及残余奥氏体含量提高、晶粒细化，致使-40 ℃冲击功增加 8.5%~24.3%、-60 ℃冲击功增加 15.6%~42.2%；此外，适当添加稀土还能改性夹杂物，生成细小弥散且与基体结合更好的复合夹杂物，通过多种机制优化熔敷金属性能。通过适量添加稀土可大幅提升 1000 MPa 级高强钢熔敷金属性能，提升熔敷金属的高强韧性匹配，满足水电用高强钢的使用需求。

关键词：1000MPa级高强钢; 熔敷金属; 埋弧焊; 稀土元素; 夹杂物

作者简介：李春剑，男，1996 年生，在读研究生，中国机械总院集团哈尔滨焊接研究所有限公司，哈尔滨 黑龙江 150028，电话：18804657650，E-mail:chumjane@126.com